INTERNATIONAL JOURNAL OF GEOMAGNETISM AND AERONOMY
VOL. 8, GI1001, doi:10.1029/2006GI000157, 2008

Formation of negative disturbances in the topside ionosphere during solar flares

L. A. Leonovich[1] and A. V. Taschilin[1]

Received 8 August 2006; revised 31 January 2007; accepted 22 April 2008; published 9 September 2008.

[1] The results of studies of the ionospheric response to solar flares are presented. The results are based on the observations of GPS signals and at incoherent scatter radars and on theoretical calculations. Analyzing the GPS data, the method based on a partial "shadowing" of the atmosphere by the Earth was used. This method made it possible to estimate the value of the electron content variations in the topside ionosphere during the solar flare on 14 July 2000. We obtained that according to the GPS data at altitudes of the topside ionosphere ($h > 300$ km) a flare is able to cause a decrease of the electron content. Similar effects of formation of a negative disturbance in the ionospheric F region were observed also during the solar flares on 21 and 23 May 1967 by the Arecibo radar. Using the theoretical model of ionosphere–plasmasphere interaction, we study in this paper the mechanism of formation of negative disturbances in the topside ionosphere during solar flares. It is shown that the intense transport of O^+ ions into the above-situated plasma caused by a sharp increase in the ion production rate and thermal expansion of the ionospheric plasma is a cause of the formation of the negative disturbance in the electron concentration in the topside ionosphere. *INDEX TERMS:* 2481 Ionosphere: Topside ionosphere; 2435 Ionosphere: Ionospheric disturbances; 2467 Ionosphere: Plasma temperature and density; *KEYWORDS:* Electron content variations; solar flare; GPS receivers network; Arecibo IS installation.

Citation: Leonovich, L. A. and A. V. Taschilin (2008), Formation of negative disturbances in the topside ionosphere during solar flares, *Int. J. Geomagn. Aeron., 8,* GI1001, doi:10.1029/2006GI000157.

1. Introduction

[2] The sharpest variations of the solar radiation fluxes ionizing the Earth's upper atmosphere occur during solar flares. A flare on the Sun presents a sudden rapid energy release in the upper chromosphere or lower corona (usually over active regions with developed groups of sunspots). A solar flare generates short-time electromagnetic radiation within the wide range of wavelengths from hard X rays with a wavelength $\lambda \sim 10^{-2}$ nm (and in some cases from gamma radiation ($\lambda \sim 10^{-4}$ nm)) to kilometer radio waves ($\lambda \sim 10^4$ m). The energy of the order of $10^{23} - 10^{25}$ J is released in powerful flares in the form of the emission. This value is much less than the total energy of the solar energy flux (more than 10^{40} J). However, for the X-ray portion of the spectrum the increase can exceed the level of the quiet sun by a factor of 10^5 [*Banks and Kockarts*, 1973; *Horan and Kreplin*, 1981]. In the ultraviolet (UV) range ($1 \le \lambda \le 100$ nm), the radiation intensity increases relatively weakly (by dozens of percents). Though relative changes of the intensity of the soft X-ray ($0.01 \le \lambda \le 1$ nm) fluxes during solar flares are much higher than in the UV spectral region, the absolute increase in the intensity of the ultraviolet radiation exceeds considerably the absolute increase in the soft X-ray radiation flux [*Krinberg and Taschilin*, 1984]. Thus, without providing any considerable input into the total solar radiation flux, a flare qualitatively changes its spectral composition. It leads to strong disturbances of the main parameters of the upper atmosphere. Ionospheric disturbances accompanying such phenomena can be included in a class of variations called sudden ionosphere disturbances or SIDs.

[3] The flare radiation could include pulse (rapid) and slow components [*Chamberlin et al.*, 2007; *Donnelly*, 1969; *Woods et al.,* 2005] emitted from the solar regions with the temperatures of $10^4 - 10^6$ K and $(1 - 30) \times 10^6$ K, respectively. In the pulse component, an increase of the UV radiation in the wavelength range 10–100 nm, X-ray radiation with the wavelengths less than 0.1 nm, and microwave radiation dominates, whereas in the slow component an increase of the X-ray radiation in the 0.1–10 nm dominates. The pulse UV radiation leads to a short-period increase in the photoioniza-

[1]Institute of Solar-Terrestrial Physics, Irkutsk, Russia

1524–4423/08/2006GI000157$18.00

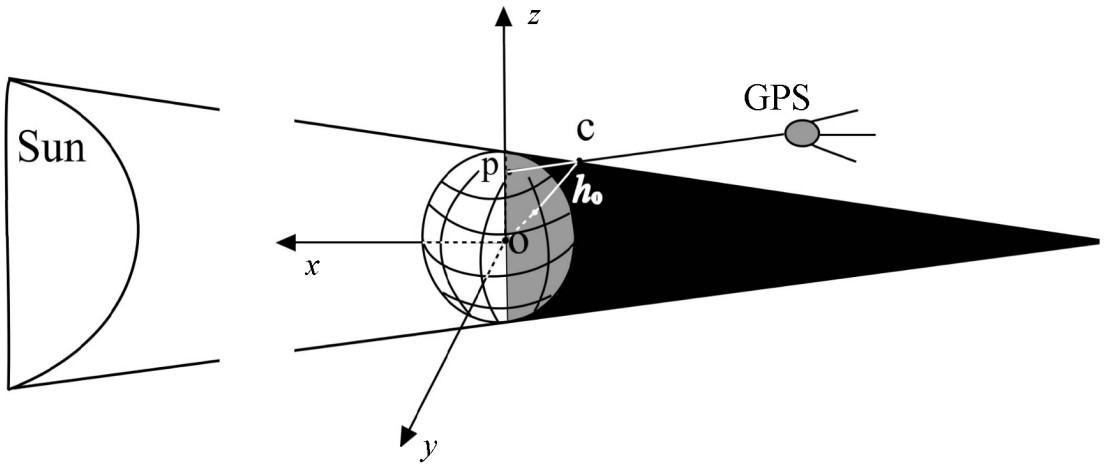

Figure 1. The scheme of the formation of the total Earth shadow cone (not scaled) in the geocentric coordinate system. Point P shows the GPS station position on the Earth's surface. C is the point in which the ray between the satellite and station crosses the boundary of the total shadow, and h_0 is the height of this point over the Earth's surface.

tion rates in the E and F ionospheric regions. The radiation within the 0.1–1.0 nm range causes a slow increase in the ionization products in the lower part of the E region and in the D region. The radiation in the 1–10 nm causes an increase in the photoionization rate at altitudes of 100–130 km.

[4] According to the observational data, the maximum increase in the electron concentration (by an order of magnitude and more) during a solar flare occurs in the ionospheric D region, whereas at altitudes of the E region, the concentration increase is by 50–200%, and in the F region it does not exceed 10–30% [*Mitra*, 1974].

[5] Currently there is no unambiguous picture of the ionospheric reaction to a solar flare within the entire height interval above 100 km. In some theoretical and experimental studies [*Koren'kov and Namgaladze*, 1977; *Liu and Lin*, 2004; *Lukicheva and Mingalev*, 1990] it was shown that the solar flare effects are manifested mainly at altitudes below the $F2$ layer, i.e., in the region were photoionization sources are located.

[6] On the other hand, there are observations [*Leonovich et al.,* 2002; *Mendillo and Evans*, 1974; *Mendillo et al.*, 1974; *Mitra*, 1974] according to which the ionosphere undergoes significant changes at altitudes exceeding considerably the $F2$-layer maximum, this fact manifests a need for detailed study of the process of redistribution of the ionospheric vertical structure during solar flares. *Koren'kov and Namgaladze* [1977] detected occurrence of negative disturbances above 300 km during solar flares.

[7] In this paper we present the results of modeling of the midlatitude ionosphere reaction at altitudes from 100 to 1000 km to the solar flare on 14 July 2000. The calculated variations of the ionospheric parameters are compared to the data on the total electron content (TEC) and electron concentration obtained at the network of the GPS receivers and incoherent scatter (IS) installations. These observations show that during the early stage of the ionospheric response to the flare, the density first decreases (negative disturbance) and then increases. The physical mechanism of formation of negative disturbances of the electron concentration in the topside ionosphere during a flare is found.

2. Observations of the TEC Variations During a Powerful Flare on 14 July 2000

[8] Phase measurements of GPS signals make it possible to obtain variations of TEC along the receiver–satellite path [*Fitzgerald*, 1997; *Hoffmann-Wellenhof et al.*, 1992; *Klobuchar*, 1987]. Assuming that the variations in TEC are the result of increased solar irradiance, it is possible to evaluate the changes in electron content above some given altitude, using the method based on the effects of partial "shadowing" of the atmosphere by the Earth. Figure 1 shows the scheme of formation of the cone of the total shadow of the Earth (out of a scale) in the geocentric solar–ecliptic coordinate system, where the z axis is directed perpendicularly to the ecliptic plane and the x axis connects the centers of the Sun and Earth. Point P marks the GPS receiver position on the Earth's surface. At the point C the ray between the satellite and reception station crosses the cone of the total shadow, h_0 being the height of this point above the Earth's surface.

[9] To study the influence of a solar flare on the ionosphere, we used the data of the GPS stations located in the vicinity of the terminator on the Earth in the nighttime hemisphere. The rays between the transmitter on board the satellite and the receiver on the Earth for these stations partially pass through the atmosphere located in the region of the total shadow and partly through the sunlit atmosphere. One can take that the measured response of TEC to a solar flare corresponds to variations in the electron content in the sunlit part of the vertical profile. This method made it possible to

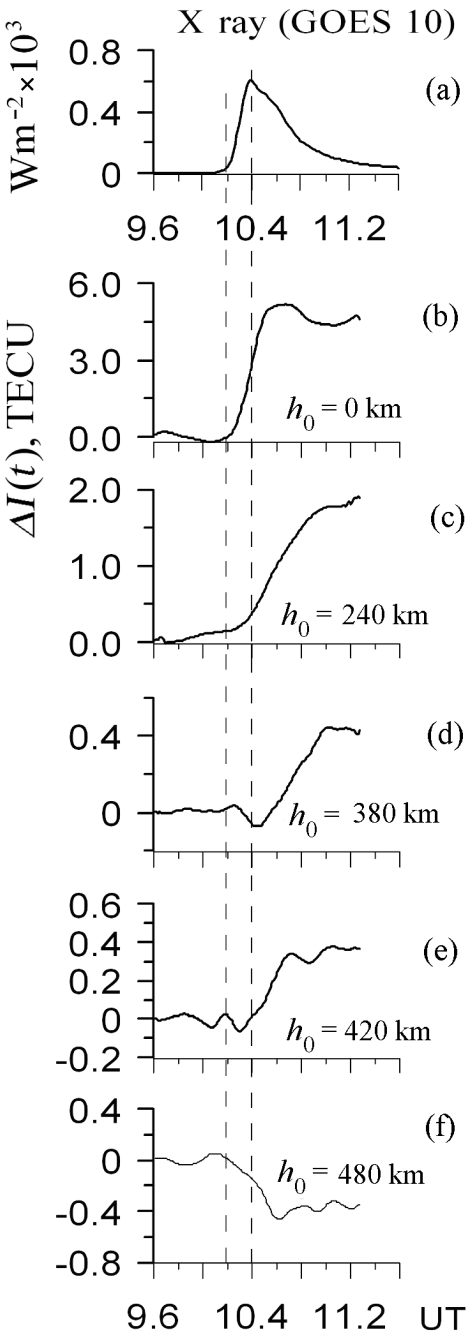

Figure 2. The results of measurements of the TEC time variations response $\Delta I(t)$ according to the GPS data. (a) Time profiles of the soft X-ray radiation within the 1–8 Å range (the data of the GOES 10 satellite) during the solar flare on 14 July 2000. (b–f) Examples of the TEC responses to the solar flare measured at the rays (between ground-based stations and GPS satellite) crossing the boundary of the Earth's shadow cone at different altitudes h_0. Vertical dashed lines show the beginning of the flare and the time when the X-ray flux was maximal.

estimate the response of the electron content to a solar flare only at altitudes of the sunlit topside ionosphere. To find the coordinates of the crossing of the ray and shadow boundary (point C in Figure 1) the system of equations was solved: the equation of the cone (of the total shadow) and equation of the line (the ray between the transmitter and receiver) given in a parametrical form. Finally it was assumed that the observed variation of the electron content along this ray is a response to a solar flare of the ionospheric region located above the h_0 level. A detailed description of the method of obtaining of the TEC excess during a solar flare was presented by *Leonovich et al.* [2002]. For measuring TEC we used the commonly accepted unit TECU equal to 10^{16} m^{-2}. The sensitivity of the phase measurements in the GPS system makes it possible to detect TEC disturbances with an amplitude as small as 10^{-3} of the background TEC value which, depending on location and local time, is from 10 to 80 TECU.

[10] Now we consider the results of application of the method described to studies of the ionospheric response to the powerful solar flare X5.7/3B registered on 14 July 2000 at 1024 UT (N22W07) on the background of quiet geomagnetic situation ($Dst = -10$ nT). Figure 2a shows the time behavior of the energy flux of the soft X rays in the 0.1–0.8 nm range (the data from the GOES 10 satellite) for the flare under consideration. Vertical dashed line show the beginning of the flare and the time when the X-ray flux was maximal. The corresponding variations in TEC $\Delta I(t)$ along rays directed to the GPS satellites and crossing the shadow boundary at various heights h_0 during the flare are shown in Figures 2b–2f. The coordinates of the receivers, GPS satellite numbers, and ray characteristics are presented in Table 1.

[11] One can see in Figure 2b that the total electron content within the entire ionosphere ($h_0 = 0$) for the IRKT station located in the sunlit hemisphere starts to grow from the moment of the flare beginning (1012 UT) and lasts till 1036 UT. At the ray crossing the shadow region at a height of 240 km (Figure 2c), the TEC grow begins some time after the flare beginning in the soft X-ray range. Similar picture is seen at other rays satisfying the condition $h_0 < 380$ km. At the same time, for the rays with $h_0 \geq 380$ km (Figures 2d–2e) a decrease in the electron content above the h_0 level occurs after the flare beginning (1012 UT) and lasts till 1024 UT, i.e., till the moment of the flare maximum in the soft X-ray range.

[12] To demonstrate that our data concerning the TEC decrease during the solar flare are correct the method of "Coherent summation" was applied to the GPS data. This method was described in detail by *Afraimovich et al.* [2001, 2002]. As the response to the solar flare appears simultaneously within the whole illuminated area this method suggests summation of the temporal responses of TEC at the GPS stations located at different points. It is clear that there is no correlation in the background fluctuations at the distances exceeding the characteristic size of irregularities. For typical duration of the UV radiation (10–15 min) associated with a solar flare the corresponding size of irregularities produced by ionization does not exceed 100 km. The distances between the GPS stations as well as the distances between the

Table 1. GPS Stations and Satellites and Parameters of the Rays Used

GPS		Station		Elevation	Azimuth	Shadow
Stations	Satellite	Latitude, deg	Longitude, deg	Angle, deg	of the Ray, deg	Height h_0, km
IRKT	23	52.219	104.316	61	268	0
FTS1	2	46.205	236.044	59	77	240
CABL	7	42.836	235.437	84	135	380
DYER	9	37.743	241.961	25	314	420
CME1	7	40.442	235.604	86	109	480

corresponding rays propagating from satellites exceed such scale. Hence, the requirement of statistical independence of the TEC fluctuations is always fulfilled. Because of summation statistically independent background fluctuations of temporal responses of TEC suppress each other. This in turn causes the increase of accuracy in measurements. In Figure 3 the averaged result of summation of the TEC variations for 15 separate rays measured by stations situated close to the terminator is presented. It is clearly seen the decrease of TEC at the initial stage of the flare.

[13] Similar decrease in the electron content after the beginning of a solar flare was detected in ionospheric observations using the incoherent scatter radar at Arecibo [*Thome and Wagner*, 1971]. During two solar flares on 21 and 23 May 1967, negative disturbances of the electron concentration with amplitudes from 3% to 10% were registered within the height interval 280–600 km.

[14] The goal of this paper is to study the mechanism of electron concentration negative disturbances in the topside ionosphere caused by solar flares.

3. Results of the Model Calculations of the Ionosphere Behavior During a Solar Flare

[15] For studying physical processes governing ionospheric effects of solar flares, we used the model of the ionosphere–plasmasphere interaction [*Krinberg and Taschilin*, 1984]. The model makes it possible to calculate time variations of the ion composition, temperature, and also of the fluxes of particles and heat in the conjugated ionospheres. The model is based on numerical solution of the nonstationary equations of the balance of particles and energy of the thermal plasma within closed magnetic field tubes, their bases lying at a height $h = 100$ km. It is assumed that the ionospheric plasma consists of electrons and atomic ions H^+ and O^+, and also of molecular ions NO^+, N_2^+, and O_2^+. The UV radiation spectrum by *Richards et al.* [1994] and the X-ray radiation spectrum by *Nusinov* [1992] were used for the calculation of the photoionization rates of the thermospheric constituents O, O_2, and N_2 and energetic spectra of the primary photoelectrons in undisturbed conditions (without a flare). The MSIS 86 [*Hedin et al.*, 1991] global empirical model of the thermosphere was used for the description of the spatial-time variations of the atmospheric temperature and concentrations of the neutral components O, O_2, N_2, and H.

[16] For studying the flare effects, a disturbed model of the solar radiation spectrum in the X-ray and UV ranges was created. According to the existence of the pulse and slow phases of a flare, we assumed that the spectrum within the wavelength interval 0.1–10 nm stays disturbed during 36 min (the slow phase), whereas the pulse phase (for the 10–105 nm interval) lasts 15 min. We also assumed that the spectrum is disturbed instantly and stays constant during the above indicated time intervals, switching off instantly after that. To give the value of the disturbance of the solar energy flux, the entire wavelength interval was split to 6 parts. For each part the most typical value of the intensity factor [*Avakyan et al.*, 1994; *Horan and Kreplin*, 1981; *Koren'kov and Namgaladze*, 1977; *Mitra*, 1974] was found. The value was determined as the ratio of the energy flux during the flare to the radiation flux of the quiet Sun. Table 2 shows values of the flare intensity factors for each spectral interval.

[17] The reaction of the midlatitude ionosphere to a considered solar flare was simulated by calculating the variations of plasma parameters within the geomagnetic field tube. The calculation was performed for the period 10–15 July 2000, using arbitrary initial conditions corresponding to low content of the thermal plasma in the tube. The considered time period was characterized by high level of solar activity ($F_{10.7} \approx 210$).

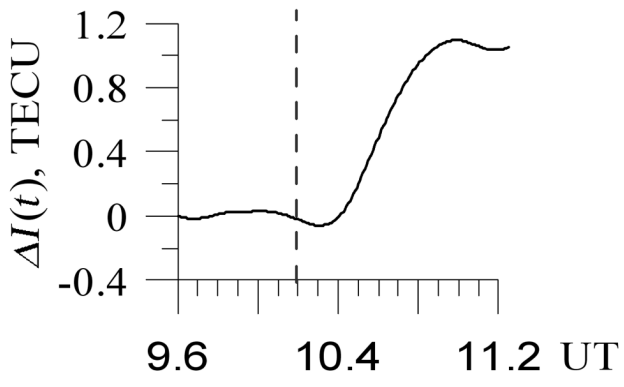

Figure 3. The averaged result of summation of the TEC time variations responses for 15 separate rays measured by the stations localized near the terminator. The moment of a solar flare beginning is shown by vertical dashed line.

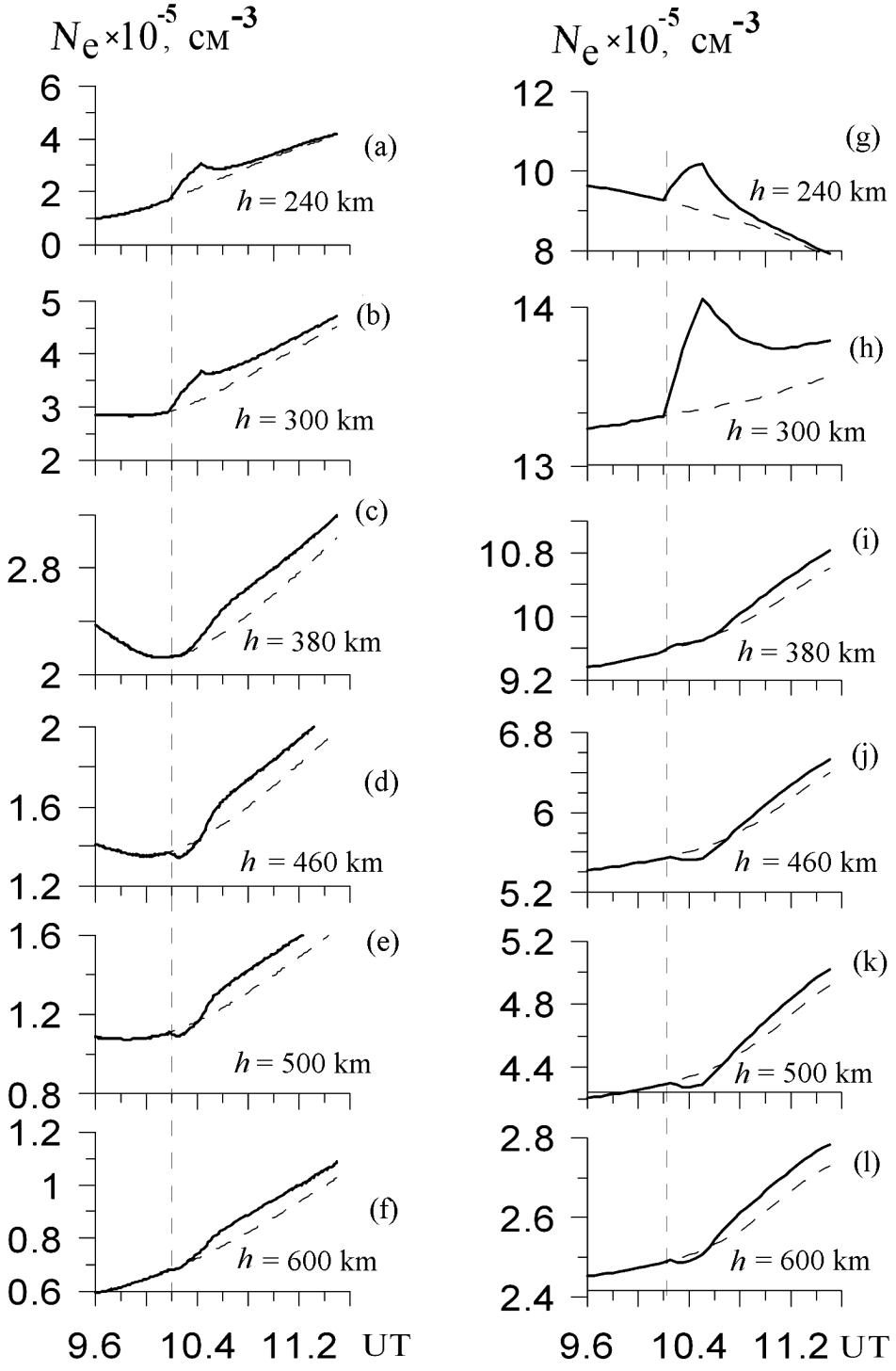

Figure 4. Model calculations of the time variations of the electron concentration at different ionospheric heights (a–f) near the terminator and (g–l) in daytime conditions. The variations of the diurnal behavior of the electron concentration in the absence of a flare are marked by dashed curves. The moment of a solar flare beginning is shown by vertical dashed lines.

[18] The results of the model calculations of the height-time variations of the electron concentration at different conditions of ionospheric illumination are presented in Figure 4 (the vicinity of the terminator (Figures 4a–4f) and local noon (Figures 4g–4l)). It is seen from Figure 4 that the variations of the electron concentration change with the height. Up to the height of 380 km the growth of the N_e concentration starts from the beginning of the solar flare (in

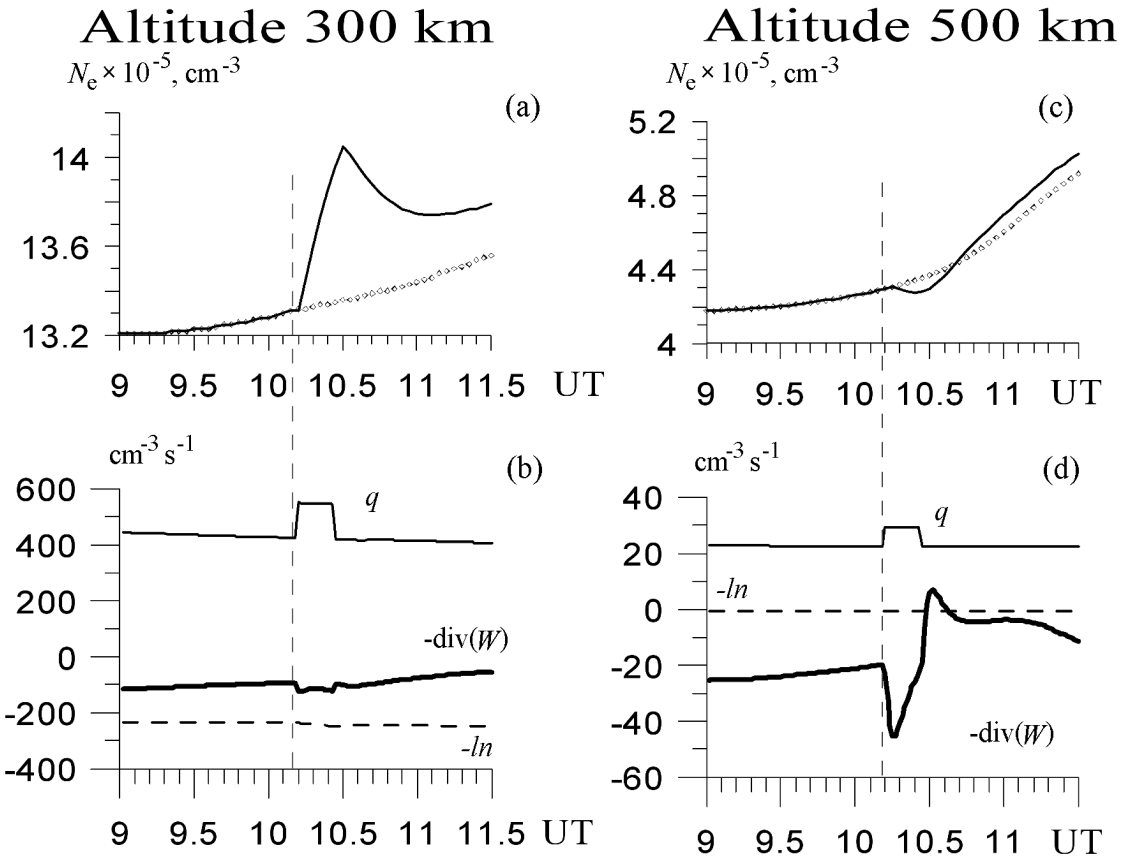

Figure 5. Analysis of the effect of the decrease in the electron concentration during the solar flare. Thick lines show the time variations of the electron concentration during a solar flare at heights of (a) 300 km and (c) 500 km, diamonds show the time variations of the electron concentration for nonflare conditions. The time variations of the terms in the continuity equation calculated for heights (b) 300 km, where the effect of the electron concentration depletion during the flare is not observed, and (d) 500 km, where the effect is clearly pronounced. The moment of the solar flare beginning is shown by vertical dashed lines.

Figure 4 the moment that corresponds to the beginning of the flare is marked by the vertical dashed lines).

[19] The character of the time behavior of N_e changes principally above the $F2$ layer. One can see in Figures 4c–4f and 4i–4l that within the height interval 380–600 km instead of the electron concentration increase after the flare beginning, a trough is formed in the time behavior of N_e, but after some period N_e starts to grow exceeding the regular value (undisturbed by the flare) of the diurnal behavior (marked by the dashed curves in Figure 4). The value of the N_e decrease amplitude lies within 1–3%. It should be noted that the obtained in the calculations negative disturbance of the electron concentration in the topside ionosphere agrees well to the presented above TEC variations obtained as a result of processing of GPS signals and in observations at the Arecibo incoherent scatter radar [*Thome and Wagner*, 1971]. Thus, one can conclude that the conditions during a solar flare could be such that an increase of the electron concentration occurs in the lower ionosphere, but in the topside ionosphere N_e decreases.

Table 2. Increase in the Solar Radiation Intensity for Particular Spectral Intervals During the Flare

	Intervals, nm					
	0.1–0.8	0.8–2	2–4	4–6	6–10	10–105
Intensity factor	1000	100	50	20	4	1.3

4. Discussion of the Modeling Results

[20] Because of the low efficiency of the impact of soft X-ray radiation (the slow phase of a flare) on the upper part of the ionosphere in the $F2$ region ($200 \leq h \leq 350$ km), the real impact is provided only by the increase in the UV radiation. So, as it follows from Figure 4g, at a height of 240 km the electron concentration increases rapidly during the pulse phase and then decreases exponentially with a characteristic time $\sim 2-3$ h. The latter value corresponds to the rate of disappearance of O^+ ions in ion-molecular reactions.

[21] In order to find the causes of formation of the electron concentration negative disturbance in the topside ionosphere, we assumed that the N_e decrease is related to inhomogeneous variations of the ultraviolet radiation in various parts of the spectrum during a flare. On the basis of this assumption, the UV radiation spectrum within the 10–105 nm range was split to 19 equal intervals. Then, for each interval in turn, the factor of flare radiation intensity changed from 1.3 to 10, whereas for the other intervals it stayed equal to 1.3. The calculations showed that the effect of N_e decrease after the beginning of a flare is pronounced best at the increase of the intensity factor in two following spectral intervals: 15–20 nm and 30–40 nm.

[22] In order to understand the physical causes of the electron concentration depletion at altitudes of the topside ionosphere, we consider the continuity equation for the ionospheric plasma written in the form

$$\frac{\partial N_e}{\partial t} = q - ln - \text{div } W \qquad (1)$$

where q is the ion production rate; ln is the loss rate of electron–ion pairs in chemical reactions; and W is the total ion flux along a geomagnetic field line. It follows from (1) that the sign of the N_e changes is determined by the total balance of the terms in the right-hand side and that a negative disturbance to be formed the right-hand side of (1) should be negative during the flare. The results of the modeling make it possible to determine the processes providing realization of such situation.

[23] Figure 5 shows the time variations of the electron concentration and particular terms of the right-hand side of equation (1) at a height of the $F2$ layer (300 km) and in the topside ionosphere (500 km). It should be noted that within this height interval ions of the atomic oxygen prevail and so equation (1) actually describe the balance of O^+ ions. It follows from Figure 5b that at a level of 300 km the value of ion production rate q exceeds considerably the loss of charged particles ln due to the recombination and transport of O^+ ions along the field lines (div $W > 0$). As a result, there occurs a monotonous increase in N_e during a flare. After the end of the flare, the photoionization rate decreases sharply. Because of that, the electron concentration at first decreases sharply and then is stabilized at some level, the latter being determined by the balance between the photoionization, input of the O^+ ions from the above-located plasmasphere, and chemical loss.

[24] At altitudes of the topside ionosphere (500 km), the relation between particular terms of the right-hand side of equation (1) is changed. First, a decrease with height in the absolute values of the ion production rates and recombination occurs, and, second, the role of the diffuse transport of ions in the ionization balance grows. Figure 5d shows that the absolute values of the divergence of ion flux rapidly increases with the beginning of the flare and becomes a predominating term in the right-hand side of equation (1). This happens due to the reformation of the vertical profile of the ion flux above the $F2$-layer maximum with the beginning of the flare.

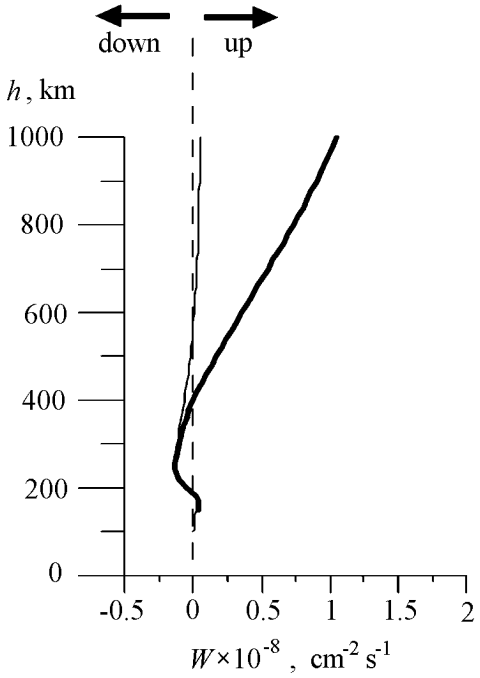

Figure 6. Vertical profile of the flux W. Thin line shows the flux behavior before the flare. Thick line shows the flux behavior during the flare.

[25] Figure 6 shows the vertical profiles of the ion flux before the flare and in the maximal phase of the flare. One can see that under undisturbed conditions ions O^+ are transported predominantly from the topside ionosphere through the $F2$ layer into the lower ionosphere. The flux of plasma upward is insignificant. This confirms that the F region and the plasmasphere are in equilibrium state. During the maximal phase of the flare, the plasma pressure in the $F2$ layer increases sharply and above ~ 380 km an intense upward flux of O^+ ions into the plasmasphere is formed. As a result, above ~ 380 km the divergence of the ion flux is positive and increases considerably by its magnitude.

[26] After the sharp increase in the initial moment of the flare, the absolute value of the flux divergence decreases reaching the preflare value at the end of the pulse phase (Figure 5d). Then a reversal of the flux divergence sign to the opposite one occurs accompanied by an increase of the electron concentration.

[27] Thus, one can conclude that the decrease of the electron concentration in the topside ionosphere is due to the

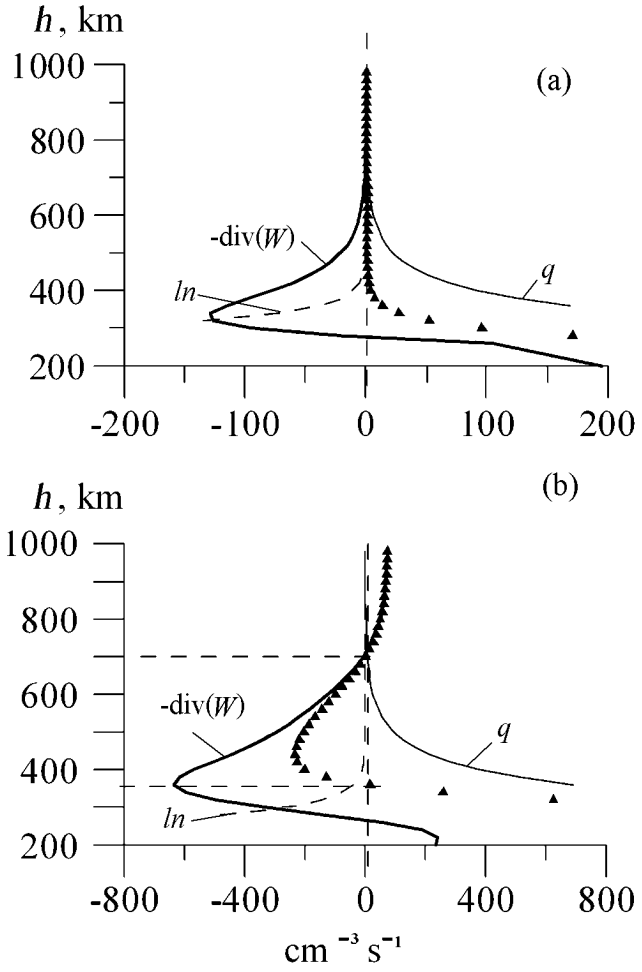

Figure 7. Analysis of the continuity equation. Vertical profiles of the terms of the continuity equation (a) before the flare and (b) during the flare. Thin curves show the electron production rate q; dashed curves show the electron loss rate ln; thick lines show the flux divergence div W. The data for the loss rate and flux divergence are shown with negative signs as they enter the considered equation. The curve with triangles is a resulting curve.

bringing out to the plasmasphere of O^+ ions. After "switching off" the flare, the plasma pressure in the $F2$ layer decreases quickly down to the level at which the difference in the pressure between the upper and lower parts of the ionosphere cannot any more support the upward flux of O^+ ions, and the ionosphere relaxes to the undisturbed state shown in Figures 5a and 5c by diamonds.

[28] Now we consider the problem of length of the height interval in which the conditions needed to formation of the negative disturbance in N_e are fulfilled. Figure 7 shows the vertical profiles of the particular terms in the right-hand side of equation (1) before a flare (Figure 7a) and during the flare (Figure 7b). In Figures 7a and 7b, the summated profile of all terms in the right-hand side of equation (1) is shown by triangles. One can see that in the absence of a solar flare in the daytime the resulting curve is positive at $h < 400$ km and is close to zero above 400 km, that is, in the topside ionosphere the condition $\partial N_e/\partial t \geq 0$ is fulfilled everywhere. During a flare the right-hand side of equation (1) takes negative values in the 380–600 km altitude range (is shown by horizontal dashed lines in Figure 7). So it follows that a negative disturbance of the electron concentration during a flare can cover almost the entire topside ionosphere.

[29] The increase in the pressure in the ionospheric $F2$ layer causing the formation of the negative disturbance of N_e in the topside ionosphere is a result of an increase in two parameters: the electron concentration and plasma temperature. The effects of N_e increase during a flare have been considered above. The rapid heating of the ionospheric plasma leads to its thermal expansion and to additional outflow of the ions into the plasmasphere, the latter process also contributing into the electron concentration depletion. So now we consider typical features of the temperature behavior during a flare. The temporal variations of the electron temperature calculated for different heights in the region of the terminator (the enhancement factor equal to 2) and during the daytime (the enhancement factor equal to 1.3) are presented in Figure 8. The temperature variations in the absence of a solar flare are marked by dashed curves The behavior of the temperature manifests the ionospheric reaction to the short-period but intense heating of the electron–ion gas. The heating energy coming from photoelectrons to one thermal electron depends slightly on the height [*Krinberg and Taschilin*, 1984] and, unlike the ion production rate, is almost constant within the entire thickness of the ionosphere. So the disturbance in T_e is developing in phase at all heights and its duration coincides with the interval of the pulse phase of the flare. The latter fact shows that the UV radiation plays the predominant role in the process of formation of the thermal response of the ionosphere above ~ 100 km. After the end of the flare, the electron temperature in the topside ionosphere gradually approaches the regular (without a flare) state.

[30] In the vicinity of the $F2$-layer maximum, the electron temperature decreases after the flare down to the values lower than the undisturbed level and then approaches the undisturbed level (Figures 8h and 8i). Such a behavior of T_e is closely related with a well-known inverse dependence of the temperature with the variations of concentration in the vicinity of the $F2$ maximum. After the end of the flare, as a result of the rapid decrease in the photoionization rate and thermal compression, an inverse flux of ions from the plasmasphere into the topside ionosphere appears. The flux maintains the increased values of the electron concentration during a few more hours. In the same time the electron temperature is decreasing because of the increase in the cooling rate under Coulomb collisions with ions and in the heat capacity of the electron–ion gas.

5. Conclusions

[31] The response of the ionosphere to a solar flare is studied on the basis of the observational data and results of the-

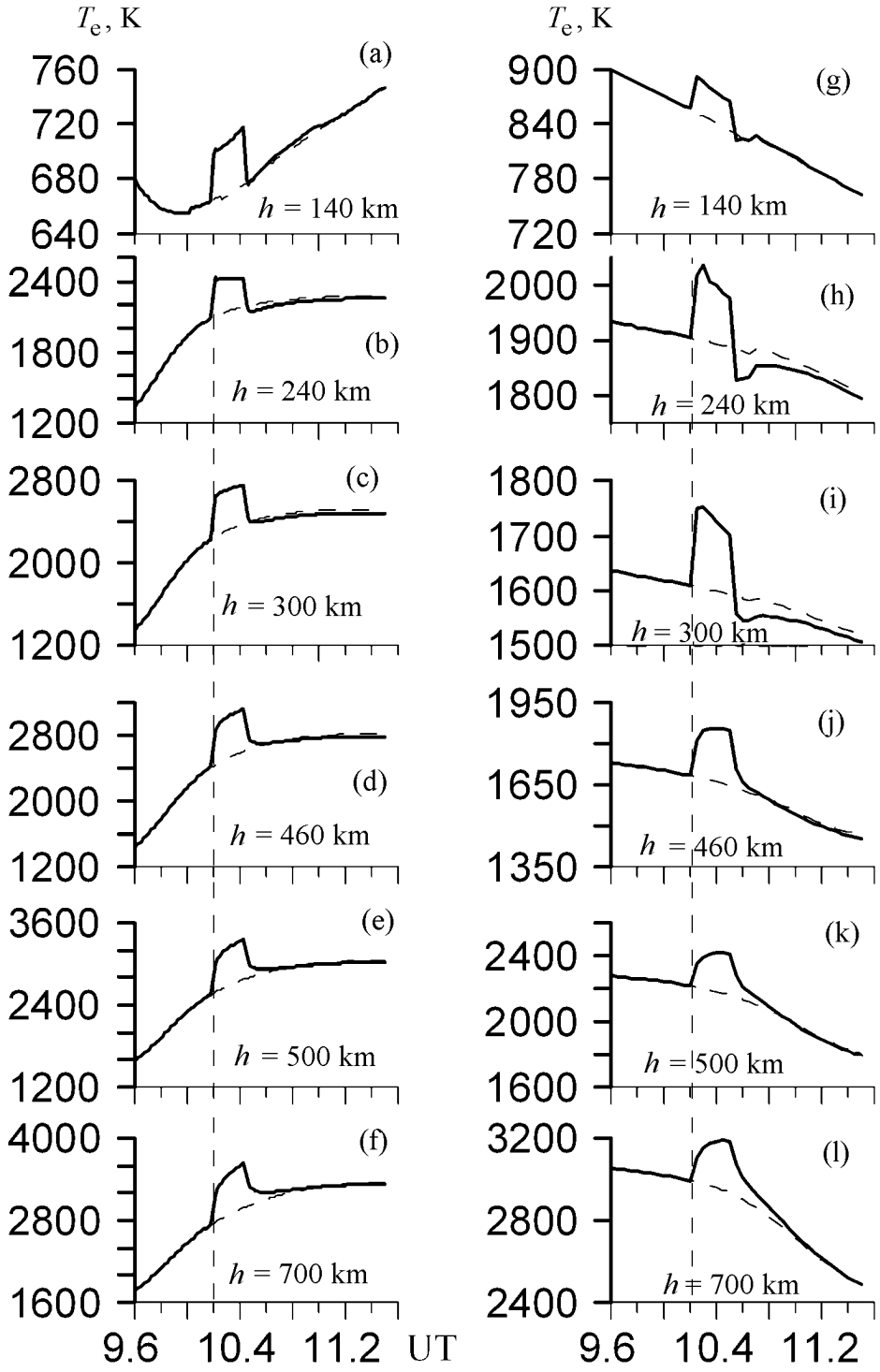

Figure 8. Time variations of the electron temperature during the flare at various heights h (solid lines) and for nonflare conditions (dashed lines) calculated for (a–f) the terminator region and (g–l) during the daytime. The moment of the solar flare is shown by vertical dashed lines.

oretical modeling. The analysis of the results obtained made it possible to draw the following conclusions:

[32] 1. According to the observations of the variations in TEC and electron concentration at the GPS receivers network and at the IS installation at Arecibo, negative disturbances of the electron concentration can be formed in the topside ionosphere during solar flares.

[33] 2. It is found in the model simulations that the most

significant effect of the N_e depletion is seen during the flares with an increase in the solar radiation within the following spectral intervals: 15–20 nm and 30–40 nm.

[34] 3. The intense transporting of O^+ ions up into the above-located plasmasphere is a cause of the formation of the negative disturbance in N_e in the topside ionosphere. The transporting is caused by the sharp increase in the ion production rate and in the thermal expansion of the ionospheric plasma.

[35] **Acknowledgments.** The GPS data on the 14 July 2000 flare were kindly provided by E. L. Afraimovich and S. V. Voeikov. E. B. Romanova helped considerably in model simulations. We sincerely thank them all.

References

Afraimovich, E. L., A. T. Altyntsev, E. A. Kosogorov, N. S. Larina, and L. A. Leonovich (2001), Ionospheric effects of the solar flares of September 23, 1998 and July 29, 1999 as deduced from global GPS network data, *J. Atmos. Sol. Terr. Phys., 63,* 1841, doi:10.1016/S1364-6826(01)00060-8.

Afraimovich, E. L., A. T. Altyntsev, V. V. Grechnev, and L. A. Leonovich (2002), The response of the ionosphere to faint and bright solar flares as deduced from global GPS network data, *Ann. Geophys., 45,* 31.

Avakyan, S. V., A. I. Vdovin, and V. F. Pustarnakov (1994), *Ionizing and Penetrating Radiation in the Near-Earth Space Environment,* 500 pp., Hydrometeoizdat, St. Petersburg, Russia.

Banks, P. M., and G. Kockarts (1973), *Aeronomy, Part A,* 144 pp., Academic, New York.

Chamberlin, P. C., T. N. Woods, and F. G. Eparvier (2007), Flare Irradiance Spectral Model (FISM): Daily component algorithms and results, *Space Weather, 5,* S07005, doi:10.1029/2007SW000316.

Donnelly, R. F. (1969), Contribution of X-ray and EUV bursts of solar flares to sudden frequency deviations, *J. Geophys. Res., 74,* 1873, doi:10.1029/JA074i007p01873.

Fitzgerald, T. J. (1997), Observations of total electron content perturbations on GPS signals caused by a ground level explosion, *J. Atmos. Sol. Terr. Phys., 59,* 829, doi:10.1016/S1364-6826(96)00105-8.

Hedin, A. E., et al. (1991), Revised global model of thermosphere winds using satellite and ground-based observations, *J. Geophys. Res., 96,* 7657, doi:10.1029/91JA00251.

Hoffmann-Wellenhof, B., H. Lichtenegger, and J. Collins (1992), *Global Positioning System: Theory and Practice,* 327 pp., Springer, Vienna, Austria.

Horan, D. M., and R. W. Kreplin (1981), Simultaneous measurements of EUV and soft X-ray solar flare emission, *Sol. Phys., 74*(1), 265, doi:10.1007/BF00151295.

Klobuchar, J. A. (1987), Ionospheric time-delay algorithm for single-frequency GPS users, *IEEE Trans. Aerosp. Electron. Syst., AES23*(3), 325, doi:10.1109/TAES.1987.310829.

Koren'kov, Yu. N., and A. A. Namgaladze (1977), Modeling of ionospheric effects of a solar flare, in *Ionospheric Disturbances and Methods of Their Forecasting* (in Russian), p. 85, Nauka, Moscow.

Krinberg, I. A., and A. V. Taschilin (1984), *Ionosphere and Plasmasphere* (in Russian), 190 pp., Nauka, Moscow.

Leonovich, L. A., E. L. Afraimovich, E. B. Romanova, and A. V. Taschilin (2002), Estimating the contribution from different ionospheric regions to the TEC response to the solar flares using data from the international GPS network, *Ann. Geophys., 20,* 1935.

Liu, J. Y., and C. H. Lin (2004), Ionospheric solar flare effects monitored by the ground-based GPS receivers: Theory and observation, *J. Geophys. Res., 109,* A01307, doi:10.1029/2003JA009931.

Lukicheva, T. N., and V. S. Mingalev (1990), Modeling of the behavior of high-latitude E and F regions of the ionosphere during solar flares, in *Studies of the Ionosphere of High Latitudes,* p. 4, Pol. Geophys. Inst., Apatity, Russia.

Mendillo, M., and J. V. Evans (1974), Incoherent scatter observations of the ionospheric response to a large solar flare, *Radio Sci., 9,* 197, doi:10.1029/RS009i002p00197.

Mendillo, M., et al. (1974), Behavior of the ionospheric F region during the great solar flare of August 7, 1972, *J. Geophys. Res., 79,* 665, doi:10.1029/JA079i004p00665.

Mitra, A. P. (1974), *Ionospheric Effects of Solar Flares,* 370 pp., D. Reidel, Boston, Mass.

Nusinov, A. A. (1992), Models for prediction of EUV- and X-ray solar radiation based on 10.7 cm radio emission, in *Proceeding of the Workshop on the Solar Electromagnetic Radiation Study for Solar Cycle 22,* p. 354, Space Environ. Lab. NOAA ERL, Boulder, Colo.

Richards, P. G., J. A. Fennelly, and D. G. Tor (1994), EUVAC: A solar EUV flux model for aeronomic calculations, *J. Geophys. Res., 99,* 8981, doi:10.1029/94JA00518.

Thome, G. D., and L. S. Wagner (1971), Electron density enhancements in the E and F regions of the ionosphere during solar flares, *J. Geophys. Res., 76,* 6883, doi:10.1029/JA076i028p06883.

Woods, T. N., F. G. Eparvier, S. M. Bailey, P. C. Chamberlin, J. Lean, G. J. Rottman, S. C. Solomon, W. K. Tobiska, and D. L. Woodraska (2005), The Solar EUV Experiment (SEE): Mission overview and first results, *J. Geophys. Res., 110,* A01312, doi:10.1029/2004JA010765.

L. A. Leonovich and A. V. Taschilin, Institute of Solar-Terrestrial Physics, P.O. Box 4026, Irkutsk, 664033 Russia. (lal@iszf.irk.ru)